Loosely Packed Self-Assembled Monolayers on Gold Generated from 2-Alkyl-2-methylpropane-1,3-dithiols

Joon-Seo Park, Aaron C. Smith, and T. Randall Lee*

Department of Chemistry, University of Houston, 4800 Calhoun Road, Houston, Texas 77204-5003

Received December 20, 2003. In Final Form: April 2, 2004

A series of 2-alkyl-2-methylpropane-1,3-dithiol derivatives with increasing alkyl chain lengths (i.e., $CH_3(CH_2)_mC(CH_3)[CH_2SH]_2$, where m = 7, 9, 11, 13, 15) were synthesized and used to generate self-assembled monolayers (SAMs) on gold. The resulting monolayers were analyzed by ellipsometry, contact angle goniometry, polarization modulation infrared reflection−absorption spectroscopy, and X-ray photoelectron spectroscopy. These data were compared with those obtained on SAMs on gold derived from normal alkanethiols ($CH_3(CH_2)_{m+2}SH$) and 2-monoalkylpropane-1,3-dithiols ($CH_3(CH_2)_mCH[CH_2SH]_2$) having the same number of carbon atoms in the primary chain. The results demonstrate that the 2-alkyl-2-methylpropane-1,3-dithiols generate conformationally disordered monolayer films in which the density of alkyl chains is less than those generated from normal alkanethiols and the 2-monoalkylpropane-1,3-dithiols.

Introduction

Controlling the interfacial properties of organic materials is critically important not only for scientific interest but also for many technological applications, particularly those that involve wetting, adhesion, corrosion prevention, and tribology.[1] In general, the surface properties of organic thin films, such as self-assembled monolayers (SAMs), can be readily manipulated by controlling the structure of the adsorbates through the use of organic synthesis. Further control over the interfacial properties of these films can be achieved by the preparation of mixed SAMs,[2−18] which can be generated on the surface of gold via the coadsorption of two distinct thiols[2−13] or the adsorption of an unsymmetrical disulfide.[14−18] Another factor that can influence the surface properties of organic thin films is the packing and orientation of the terminal functional groups. For example, SAMs generated from normal alkanethiols on GaAs(100) possess an average chain tilt angle of 57°, which is distinct from that of SAMs on gold (30°).[19] Correspondingly, *n*-alkanethiolate SAMs on GaAs(100) exhibit lower contact angles of hexadecane than do analogous SAMs on gold. The lower value can be rationalized by the partial exposure of interfacial methylene groups on the SAMs having the greater chain tilt.

Controlling the conformation of the adsorbates offers an additional avenue for manipulating the interfacial properties and/or reactivities of SAMs. Harder and coworkers showed that the conformation of the tail groups in oligo(ethylene glycol)-terminated SAMs can influence the resistance to protein adsorption onto the surface.[20] While SAMs having oligo(ethylene glycol) moieties with helical (gauche−trans−gauche) or amorphous conformations were resistant to protein absorption, the densely packed analogue in an all-trans conformation was found to adsorb proteins. The results were rationalized on the basis of a conformation-dependent degree of solvation. Even for identical methoxy-terminated ethylene glycol adsorbates, the selection of the substrate (e.g., gold vs silver) influenced the conformation of the tail groups and thus protein adsorption. For hydrocarbon SAMs, the alkyl chains are typically densely packed and exist in a trans-extended conformation. One immediate goal of our research is to develop strategies for precisely controlling the conformations of hydrocarbon SAMs; a more long term goal seeks to extend these strategies to various functionalized SAMs, including those that resist the adsorption of proteins, cells, and other biologically relevant materials.

Hydrocarbon SAMs having a low packing density of alkyl chains are known to be conformationally disordered.[21] We anticipate that the degree of conformational disorder can be controlled by carefully regulating the packing densities of the adsorbates. Since the surface properties of polymer films are determined by the outmost 5−10 Å,[1,22] loosely packed SAMs can be used as model

* To whom correspondence should be addressed. E-mail: trlee@uh.edu.

(1) Ulman, A. *Chem. Rev.* **1996**, *96*, 1533.
(2) Bain, C. D.; Whitesides, G. M. *J. Am. Chem. Soc.* **1988**, *110*, 6560.
(3) Bain, C. D.; Evall, J.; Whitesides, G. M. *J. Am. Chem. Soc.* **1989**, *111*, 7155.
(4) Bain, C. D.; Whitesides, G. M. *J. Am. Chem. Soc.* **1989**, *111*, 7164.
(5) Folkers, J. P.; Laibinis, P. E.; Whitesides, G. M. *Langmuir* **1992**, *8*, 1330.
(6) Folkers, J. P.; Laibinis, P. E.; Whitesides, G. M.; Deutch, J. *J. Phys. Chem.* **1994**, *98*, 563.
(7) Ulman, A. *Thin Solid Films* **1996**, *273*, 48.
(8) Tamada, K.; Hara, M.; Sasabe, H.; Knoll, W. *Langmuir* **1997**, *13*, 1558.
(9) Imabayashi, S.; Hobara, D.; Kakiuchi, T.; Knoll, W. *Langmuir* **1997**, *13*, 4502.
(10) Lingyan, L.; Shengfu, C.; Shaoyi, J. *Langmuir* **2003**, *19*, 666.
(11) Lingyan, L.; Shengfu, C.; Shaoyi, J. *Langmuir* **2003**, *19*, 3266.
(12) Lahiri, J.; Isaacs, L.; Tien, J.; Whitesides, G. M. *Anal. Chem.* **1999**, *71*, 777.
(13) Qian, X.; Metallo, S. J.; Choi, I. S.; Wu, H.; Liang, M. N.; Whitesides, G. M. *Anal. Chem.* **2002**, *74*, 1805.
(14) Biebuyck, H. A.; Whitesides, G. M. *Langmuir* **1993**, *9*, 1766.
(15) Schoenherr, H.; Ringsdorf, H. *Langmuir* **1996**, *12*, 3891.
(16) Higashi, N.; Takahashi, M.; Niwa, M. *Langmuir* **1999**, *15*, 111.
(17) Azehara, H.; Yoshimoto, S.; Hokari, H.; Akiba, U.; Taniguchi, I.; Fujihira, M. *J. Electroanal. Chem.* **1999**, *473*, 68.
(18) Tsao, M.-W.; Rabolt, J. F.; Schoenherr, H.; Castner, D. G. *Langmuir* **2000**, *16*, 1734.
(19) Sheen, C. W.; Shi, J.-X.; Martensson, J.; Parikh, A. N.; Allara, D. L. *J. Am. Chem. Soc.* **1992**, *114*, 1514.
(20) Harder, P.; Grunze, M.; Dahint, R.; Whitesides, G. M.; Laibinis, P. E. *J. Phys. Chem. B* **1998**, *102*, 426.
(21) Shon, Y.-S.; Colorado, R., Jr.; Williams, C. T.; Bain, C. D.; Lee, T. R. *Langmuir* **2000**, *16*, 541.
(22) Allara, D. L. In *Polymer Surfaces and Interfaces*; Feast, W. J., Munro, H. S., Richards, R. W., Eds.; Wiley: Chichester, 1993; Vol. II, p 27.

10.1021/la036424z CCC: $27.50
Published on Web 05/29/2004

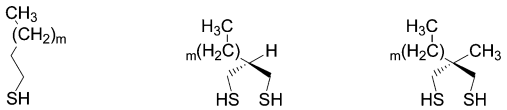

m = 7	**C10**	**C10C2**	**C10C3**
m = 9	**C12**	**C12C2**	**C12C3**
m = 11	**C14**	**C14C2**	**C14C3**
m = 13	**C16**	**C16C2**	**C16C3**
m = 15	**C18**	**C18C2**	**C18C3**
	Cn	***CnC2***	***CnC3***

Figure 1. Structures of normal alkanethiols (**C*n***), the corresponding 2-monoalkylpropane-1,3-dithiols (**C*n*C2**), and the corresponding 2-alkyl-2-methylpropane-1,3-dithiols (**C*n*C3**), where $m = 7, 9, 11, 13, 15$ (and thus $\boldsymbol{n} = 10, 12, 14, 16, 18$). For a given value of ***n***, the number of carbon atoms from the sulfur atom to the terminal methyl group of the longest chain is the same for all three classes of adsorbate.

surfaces of polymer films (e.g., the surfaces of proteins and amorphous polymers), which are typically conformationally complex rather than ordered.[23] Another interesting feature of loosely packed SAMs is their potential to intercalate guest molecules into void spaces between the chains of the adsorbates. This feature promises a variety of applications. For example, control over the lateral density of anthryl groups can be used to promote the immobilization of DNA via intercalation.[24,25] This type of intercalation, which is likely facilitated solely by van der Waals interactions, offers a unique strategy for controlling the composition and inherent properties of interfaces (e.g., wetting, adhesion, and molecular recognition).

Recently, our research has targeted the preparation and study of low-density SAMs on gold generated from 2-monoalkylpropane-1,3-dithiols (**C*n*C2**, Figure 1) and structurally related adsorbates.[21,26−29] These chelating alkanedithiols can be used to prepare well-defined model interfaces that are conformationally disordered because the alkyl chains are loosely packed on gold substrates. The resultant liquidlike films exhibit greater wettabilities and frictional responses than conformationally ordered monolayers derived from normal alkanethiols (**C*n***).[21,26,27,30] In addition, studies of monolayer desorption and exchange showed an enhanced thermodynamic stability for these chelating SAMs when compared to analogous *n*-alkanethiolate SAMs; the enhanced stability was rationalized on the basis of the chelate effect and the ring strain generated in the formation of cyclic disulfide desorption products.[28] Further comparison of these low-density SAMs to branched and linear polyethylene films, however, suggested that the interfacial structure/composition of the 2-monoalkylpropane-1,3-dithiol SAMs is more similar to that of densely packed *n*-alkanethiolate SAMs than to that of hydrocarbon polymer films.[21] The preparation of appropriate polymer-surface mimics from loosely packed but well-defined SAMs, therefore, remains a continuing goal of our research.

In this report, we describe a new series of well-defined SAMs generated from 2-alkyl-2-methylpropane-1,3-dithiols (**C*n*C3**), which are designed to exhibit an even lower density of alkyl chains than those derived from **C*n*C2**. We reasoned that SAMs of **C*n*C3** would have a lower density of alkyl chains than those derived from **C*n*C2** because of the steric bulk of the methyl group near the quaternary carbon center. This expectation was suggested by the study of wettabilities and frictional properties of SAMs generated from spiroalkanedithiols (**C*n*C*m***), in which one of the two alkyl chain lengths was systematically varied.[26] Consequently, we anticipated SAMs generated from **C*n*C3** would be more conformationally disordered than those generated from either **C*n*** or **C*n*C2**. Additionally, we anticipated a homogeneously mixed array of alkyl chains, as was observed for related dithiol systems.[29]

Specifically, this paper describes the synthesis of a series of **C*n*C3** adsorbates and their use to prepare loosely packed SAMs on gold (Figure 2). The resulting monolayers were analyzed by ellipsometry, contact angle goniometry, polarization modulation infrared reflection−absorption spectroscopy (PM-IRRAS), and X-ray photoelectron spectroscopy (XPS). These data were compared with those obtained from SAMs derived from **C*n*** and **C*n*C2** having corresponding numbers of carbon atoms along the primary chain (i.e., from the sulfur atom to the terminal methyl group).

Experimental Section

Materials and Methods. Gold shot (99.99%) was purchased from Americana Precious Metals, and polished single-crystal silicon (111) wafers were purchased from NESTEC. Dimethylformamide (DMF), triethylamine (Et_3N), and tetrahydrofuran (THF) were purchased from EM Sciences; THF was dried by passage through alumina before use. Dimethyl sulfoxide (DMSO), diethyl malonate, sodium hydride (NaH), iodomethane (CH_3I), and lithium aluminum hydride (LAH) were purchased from Aldrich Chemical Co. and used as received. DMSO was dried over calcium hydride and then distilled and stored under argon. Methanesulfonyl chloride and potassium thioacetate (KSAc) were purchased from Acros and used as received. The starting bromoalkanes were of the highest purity available from Aldrich Chemical Co. Column chromatography was performed using silica gel (60−200 mesh) purchased from Natland International. Thin-layer chromatography (TLC) was carried out using 250-mm-thick Whatman silica gel plates. The eluted TLC plates were analyzed in an iodine chamber. Nuclear magnetic resonance (NMR) spectra were recorded on a General Electric QE-300 spectrometer operating at 300 MHz for ^1H and 75 MHz for ^{13}C nuclei. The data were obtained in $CDCl_3$ and referenced to δ 7.26 for ^1H and δ 77.23 for ^{13}C spectra. Elemental analyses were performed by Chemisar Laboratories, Inc.

Synthesis of 2-Alkyl-2-methylpropane-1,3-dithiols. The strategy used to synthesize the 2-alkyl-2-methylpropane-1,3-dithiols, **C*n*C3**, is shown in Scheme 1. We provide a description of all materials and synthetic methods as well as complete experimental details of each synthetic step by using the synthesis of **C16C3** as an illustrative example. We also provide complete analytical data for all dithiol final products. Please note that the synthesis methods and analytical data for 2-dodecylpropane-1,3-dithiol (**C14C2**) and 2-tetradecylpropane-1,3-dithiol (**C16C2**) have been provided in a previous report.[21]

*Diethyl 2-Tetradecylmalonate (**1**).* A solution of NaH (2.60 g, 65 mmol; 60% dispersion in mineral oil) in THF (75 mL) and DMF (25 mL) was prepared at 0 °C under an atmosphere of nitrogen. To this stirred solution maintained at 0 °C, diethyl malonate (8.01 g, 50.0 mmol) was added slowly. Stirring was

(23) Bain, C. D.; Whitesides, G. M. *Angew. Chem., Int. Ed. Engl.* **1989**, *28*, 506.
(24) Higashi, N.; Takahashi, M.; Niwa, M. *Langmuir* **1999**, *15*, 111.
(25) Nakamura, F.; Mitsui, K.; Hara, M.; Kraemer, S.; Mittler, S.; Knoll, W. *Langmuir* **2003**, *19*, 5823.
(26) Shon, Y.-S.; Lee, S.; Colorado, R., Jr.; Perry, S. S.; Lee, T. R. *J. Am. Chem. Soc.* **2000**, *122*, 7556.
(27) Lee, S.; Shon, Y.-S.; Colorado, R., Jr.; Guenard, R. L.; Lee, T. R.; Perry, S. S. *Langmuir* **2000**, *16*, 2220.
(28) Shon, Y.-S.; Lee, T. R. *J. Phys. Chem. B* **2000**, *104*, 8192.
(29) Shon, Y.-S.; Lee, S.; Perry, S. S.; Lee, T. R. *J. Am. Chem. Soc.* **2000**, *122*, 1278.
(30) Ulman, A. *An Introduction to Ultrathin Organic Films*; Academic: Boston, 1991.

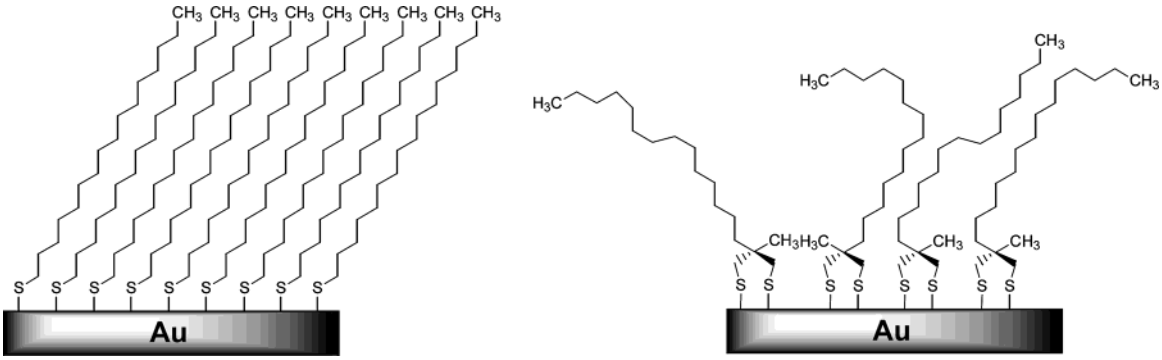

Figure 2. Schematic representations of (left) a densely packed SAM derived from **C16** and (right) a loosely packed SAM derived from **C16C3**.

Scheme 1

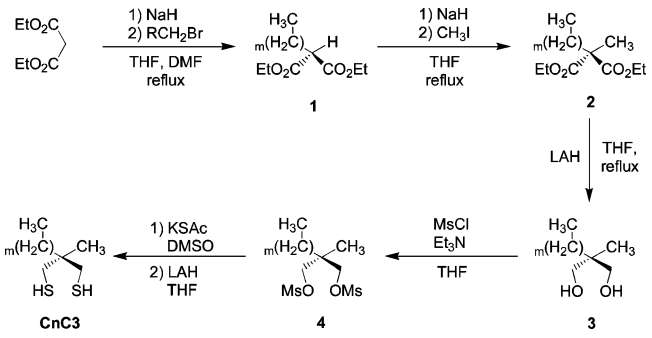

continued for 15 min at room temperature, and then bromotetradecane (14.56 g, 52.51 mmol) was added. The reaction mixture was heated under reflux for 5 h and then concentrated under reduced pressure. The resultant oil was suspended in water (100 mL) and extracted with hexanes (2 × 150 mL) and then a 1:1 mixture of hexanes and diethyl ether (1 × 150 mL). The combined organic layers were washed with water (2 × 100 mL), dried over $MgSO_4$, filtered, and concentrated under reduced pressure. The mixture was purified by column chromatography (hexanes/diethyl ether, 5/1) to give a colorless oil (11.00 g, 30.85 mmol; 62%). ^{1}H NMR (300 MHz, $CDCl_3$): δ 4.19 (q, J = 7.2 Hz, 4 H, OCH_2), 3.30 (t, J = 7.6 Hz, 1 H, C(O)C*H*), 1.88 (m, 2 H, CH_2CH), 1.38−1.20 (m, 30 H), 0.88 (t, J = 6.5 Hz, 3 H, CH_3).

*Diethyl 2-Methyl-2-tetradecylmalonate (**2**).* NaH (0.77 g, 19 mmol) was placed in a dry nitrogen-flushed flask, and THF (75 mL) and DMF (25 mL) were transferred into the flask at 0 °C under an atmosphere of nitrogen. To this solution maintained at 0 °C, diester **1** (4.55 g, 12.8 mmol) was added slowly. The mixture was stirred at room temperature for 15 min, and then iodomethane (1.20 mL, 19.3 mmol) was transferred into the mixture via syringe. The reaction mixture was heated under reflux for 5 h and then concentrated under a vacuum. The resultant oil was suspended in water (100 mL) and extracted with hexanes (2 × 100 mL) and then a 1:1 mixture of hexanes and diethyl ether (1 × 150 mL). The organic layers were washed with water (2 × 70 mL), dried over $MgSO_4$, and filtered. Removal of solvents under a vacuum afforded a colorless oil of crude diethyl 2-methyl-2-tetradecylmalonate (4.41 g, 11.9 mmol; 93%). ^{1}H NMR (300 MHz, $CDCl_3$): δ 4.17 (q, J = 7.1 Hz, 4 H, OCH_2), 1.83 (m, 2 H, CH_2C), 1,39 (s, 3 H, CH_3C), 1.35−1.18 (m, 30 H), 0.88 (t, J = 6.8 Hz, 3 H, CH_3).

*2-Methyl-2-tetradecylpropane-1,3-diol (**3**).* A solution of diester **2** (4.28 g, 11.5 mmol) in THF (100 mL) was prepared under an atmosphere of nitrogen. To this solution was added slowly lithium aluminum hydride (1.75 g, 46.1 mmol). The reaction mixture was refluxed for 3 h under a nitrogen atmosphere, quenched with ethanol (25 mL), and acidified to ca. pH 1 by careful addition of 1 M HCl solution (150 mL). The mixture was extracted with diethyl ether (3 × 100 mL). The organic layers were washed with a dilute HCl solution (1 × 100 mL) and brine (1 × 100 mL) and then dried over $MgSO_4$ and filtered. The solvent was removed under a vacuum to give crude 2-tetradecylpropane-1,3-diol as an oil (3.13 g, 10.9 mmol; 95%). ^{1}H NMR (300 MHz, $CDCl_3$): δ 3.54 (m, 4 H, CH_2OH), 1.46−1.20 (m, 26 H), 0.88 (t, J = 6.5 Hz, 3 H, CH_3), 0.83 (s, 3 H, CH_3C).

*2-Methyl-2-tetradecylpropane-1,3-dimesylate (**4**).* Methanesulfonyl chloride (3.12 g, 27.3 mmol) was added dropwise over 5 min to a solution of diol **3** (3.11 g, 10.9 mmol) and triethylamine (2.76 g, 27.3 mmol) in THF (100 mL). The reaction mixture was stirred at room temperature for 4 h. Ice-cold water (100 mL) was poured into the flask to destroy any excess methanesulfonyl chloride. The aqueous layer was separated from the organic layer and extracted with dichloromethane (3 × 100 mL). The combined organic phases were washed with dilute HCl (1 × 100 mL), water (1 × 100 mL), $NaHCO_3$ solution (1 × 100 mL), and water (1 × 100 mL). The organic layer was dried over $MgSO_4$, filtered, and concentrated to dryness to afford crude 2-methyl-2-tetradecylpropane-1,3-dimesylate (4.54 g, 10.3 mmol; 94%). ^{1}H NMR (300 MHz, $CDCl_3$): δ 4.05 (d, J = 9.7 Hz, 2 H, CH_2OMs), 4.01 (d, J = 9.7 Hz, 2 H, CH_2OMs), 3.04 (s, 6 H, O*Ms*), 1.41−1.20 (m, 26 H), 1.01 (s, 3 H, CH_3C), 0.88 (t, J = 6.5 Hz, 3 H, CH_3).

*2-Methyl-2-tetradecylpropane-1,3-dithiol (**C16C3**).* Dimesylate **4** (4.50 g, 10.2 mmol) was dissolved in DMSO (70 mL). Potassium thioacetate (2.91 g, 25.5 mmol) was added to the solution, and the reaction mixture was heated to 100 °C for 24 h under an atmosphere of nitrogen. Brine (150 mL) was poured into the solution, and the mixture was extracted with diethyl ether (3 × 100 mL). The organic phases were combined and washed with brine (2 × 100 mL). The organic layer was dried over $MgSO_4$, filtered, and evaporated to dryness. The crude products were placed in THF (80 mL), and lithium aluminum hydride (1.55 g, 40.8 mmol) was added slowly at room temperature. The reaction mixture was refluxed for 3 h under an atmosphere of nitrogen and then quenched with ethanol (25 mL). The mixture was acidified to ca. pH 1 by careful addition of 1 M HCl solution (150 mL) and then extracted with diethyl ether (3 × 100 mL). The organic layers were combined and then washed with a dilute HCl solution (3 × 100 mL) and brine (1 × 100 mL). The organic phase was dried over $MgSO_4$ and filtered. After removal of the volatiles under a vacuum, the crude products were purified by column chromatography on silica gel (hexanes/diethyl ether, 1/0 → 20/1), affording 2-methyl-2-tetradecylpropane-1,3-dithiol (1.50 g, 4.70 mmol; 46%). ^{1}H NMR (300 MHz, $CDCl_3$): δ 2.55 (B part of ABX system, J_{AB} = 13.8 Hz, J_{AX} = 8.8 Hz, 2 H, SCH_2), 2.52 (A part of ABX system, J_{AB} = 13.8 Hz, J_{AX} = 8.8 Hz, 2 H, SCH_2), 1.37−1.19 (m, 26 H), 1.15 (t, J = 8.8 Hz, 2 H, S*H*), 0.94 (s, 3 H, CH_3C), 0.88 (t, J = 6.7 Hz, 3 H, CH_3CH$_2$). ^{13}C NMR (75 MHz, $CDCl_3$): δ 37.74, 37.38, 32.99, 32.13, 30.53, 29.89, 29.87, 29.81, 29.57, 23.85, 22.89, 22.65, 14.32. Anal. Calcd for $C_{18}H_{38}S_2$: C, 67.85; H, 12.02. Found: C, 67.49; H, 12.20.

*2-Octyl-2-methylpropane-1,3-dithiol (**C10C3**).* ^{1}H NMR (300 MHz, $CDCl_3$): δ 2.55 (B part of ABX system, J_{AB} = 13.8 Hz, J_{AX} = 8.7 Hz, 2 H, SCH_2), 2.52 (A part of ABX system, J_{AB} = 13.8 Hz, J_{AX} = 8.7 Hz, 2 H, SCH_2), 1.38−1.19 (m, 14 H), 1.15 (t, J = 8.7 Hz, 2 H, S*H*), 0.94 (s, 3 H, CH_3C), 0.88 (t, J = 6.7 Hz, 3 H, CH_3CH$_2$). ^{13}C NMR (75 MHz, $CDCl_3$): δ 37.78, 37.40, 33.02, 32.10, 30.54, 29.78, 29.52, 23.88, 22.89, 22.69, 14.34. Anal. Calcd for $C_{12}H_{26}S_2$: C, 61.47; H, 11.18. Found: C, 61.50; H, 11.41.

*2-Decyl-2-methylpropane-1,3-dithiol (**C12C3**).* ^{1}H NMR (300 MHz, $CDCl_3$): δ 2.55 (B part of ABX system, J_{AB} = 13.7 Hz, J_{AX} = 8.7 Hz, 2 H, SCH_2), 2.52 (A part of ABX system, J_{AB} = 13.7 Hz, J_{AX} = 8.7 Hz, 2 H, SCH_2), 1.38−1.18 (m, 18 H), 1.15 (t, J =

8.7 Hz, 2 H, SH), 0.94 (s, 3 H, CH_3C), 0.88 (t, J = 6.7 Hz, 3 H, CH_3CH_2). ^{13}C NMR (75 MHz, $CDCl_3$): δ 37.77, 37.37, 32.99, 32.13, 30.53, 29.84, 29.56, 23.88, 22.92, 22.67, 14.38. HRMS Calcd for $C_{14}H_{30}S_2$: 262.1789. Found: 262.1786.

*2-Dodecyl-2-methylpropane-1,3-dithiol (**C14C3**).* ^{1}H NMR (300 MHz, $CDCl_3$): δ 2.55 (B part of ABX system, J_{AB} = 13.8 Hz, J_{AX} = 8.7 Hz, 2 H, SCH_2), 2.52 (A part of ABX system, J_{AB} = 13.8 Hz, J_{AX} = 8.7 Hz, 2 H, SCH_2), 1.37−1.20 (m, 22 H), 1.15 (t, J = 8.7 Hz, 2 H, SH), 0.94 (s, 3 H, CH_3C), 0.88 (t, J = 6.7 Hz, 3 H, CH_3CH_2). ^{13}C NMR (75 MHz, $CDCl_3$): δ 38.16, 37.79, 33.41, 32.55, 30.95, 30.27, 29.98, 24.27, 23.32, 23.07, 14.75. Anal. Calcd for $C_{16}H_{34}S_2$: C, 66.14; H, 11.79. Found: C, 66.18; H, 12.23.

*2-Hexadecyl-2-methylpropane-1,3-dithiol (**C18C3**).* ^{1}H NMR (300 MHz, $CDCl_3$): δ 2.55 (B part of ABX system, J_{AB} = 13.8 Hz, J_{AX} = 8.7 Hz, 2 H, SCH_2), 2.52 (A part of ABX system, J_{AB} = 13.8 Hz, J_{AX} = 8.7 Hz, 2 H, SCH_2), 1.37−1.20 (m, 30 H), 1.15 (t, J = 8.7 Hz, 2 H, SH), 0.94 (s, 3 H, CH_3C), 0.88 (t, J = 6.7 Hz, 3 H, CH_3CH_2). ^{13}C NMR (75 MHz, $CDCl_3$): δ 37.75, 37.39, 33.00, 32.14, 30.54, 29.91, 29.58, 23.86, 22.90, 22.66, 14.33. Anal. Calcd for $C_{20}H_{42}S_2$: C, 69.29; H, 12.21. Found: C, 69.60; H, 12.45.

*2-Octylpropane-1,3-dithiol (**C10C2**).* ^{1}H NMR (300 MHz, $CDCl_3$): δ 2.77−2.58 (m, 4 H, SCH_2), 1.67 (m, 1 H, CH), 1.42−1.20 (m, 14 H), 1.20 (t, J = 8.4 Hz, 2 H, SH), 0.88 (t, J = 6.6 Hz, 3 H, CH_3). ^{13}C NMR (75 MHz, $CDCl_3$): δ 42.85, 32.09, 31.67, 29.94, 29.73, 29.49, 27.10, 26.97, 22.89, 14.32. Anal. Calcd for $C_{11}H_{24}S_2$: C, 59.94; H, 10.97. Found: C, 59.92; H, 11.21.

*2-Decylpropane-1,3-dithiol (**C12C2**).* ^{1}H NMR (300 MHz, $CDCl_3$): δ 2.82−2.58 (m, 4 H, SCH_2), 1.67 (m, 1 H, CH), 1.41−1.21 (m, 18 H), 1.20 (t, J = 8.4 Hz, 2 H, SH), 0.88 (t, J = 6.7 Hz, 3 H, CH_3). ^{13}C NMR (75 MHz, $CDCl_3$): δ 42.79, 32.01, 31.33, 29.79, 29.67, 28.83, 28.24, 27.01, 26.95, 22.86, 15.13. HRMS Calcd for $C_{13}H_{28}S_2$: 248.1632. Found: 248.1631.

*2-Hexadecylpropane-1,3-dithiol (**C18C2**).* ^{1}H NMR (300 MHz, $CDCl_3$): δ 2.76−2.57 (m, 4 H, SCH_2), 1.67 (m, 1 H, CH), 1.40−1.19 (m, 30 H), 1.19 (t, J = 8.3 Hz, 2 H, SH), 0.88 (t, J = 6.7 Hz, 3 H, CH_3). ^{13}C NMR (75 MHz, $CDCl_3$): δ 42.86, 32.14, 31.68, 29.91, 29.83, 29.77, 29.58, 27.09, 26.97, 22.91, 14.33. Anal. Calcd for $C_{19}H_{40}S_2$: C, 68.60; H, 12.12. Found: C, 68.78; H, 12.52.

Preparation of SAMs. The gold substrates were prepared by the thermal evaporation of 1000 Å of gold onto silicon wafers at a rate of 1 Å/s in a diffusion-pumped chamber at ca. 1×10^{-5} Torr.[31] The silicon wafers were precoated with 100 Å of chromium to promote the adhesion of gold. The evaporation rates and thicknesses were monitored with a quartz oscillator. Upon completion of the evaporation, the cryogenically pumped chamber was cooled to room temperature and backfilled with ultrapure nitrogen. The silicon wafers were cut into slides (ca. 1 × 4 cm) with a diamond-tipped stylus, and the slides were rinsed with ethanol and dried with a stream of ultrapure nitrogen before use. The SAMs were prepared by immersing the slides in ethanolic solutions containing the appropriate thiols at 1 mM concentrations. The vials containing the solutions were precleaned in "piranha" solution (3:1, H_2SO_4/H_2O_2) for 1 h, exhaustibly rinsed with deionized water and ethanol, and then dried in an oven at ~100 °C. (*Caution*: *Piranha solution is extremely hazardous*; *it should be handled with great care and never stored in a sealed container*.) The gold-coated silicon wafers were immersed in the solutions and allowed to equilibrate for 48 h. After SAM formation, the slides were rinsed thoroughly with toluene and ethanol and dried by exposure to a vigorous stream of ultrapure nitrogen before characterization.

Ellipsometric Thickness Measurements. The thicknesses of the monolayers were measured using a Rudolf Research Auto EL III ellipsometer equipped with a He−Ne laser operating at 632.8 nm and an incident angle of 70°. The optical constants of the bare gold substrates were measured immediately after the evaporation of gold. To calculate the thicknesses of the monolayers, a refractive index of 1.45 was assumed for all films. The data were collected and averaged from measurements on at least three separate slides using three spots per slide for each type of monolayer film. The measured ellipsometric thicknesses were always within ±1 Å of the reported values.

(31) At this pressure, evaporation rates faster than 1 Å/s yielded gold substrates with relatively poor quality as judged by ellipsometric constants and the contact angle measurements of subsequently prepared SAMs.

Contact Angle Measurements. Contact angles of hexadecane and water were measured at room temperature and ambient relative humidity using a Ramé-Hart model 100 contact angle goniometer. The contacting liquids were dispensed (advancing) and withdrawn (receding) at the slowest possible speed (~1 μL/s) using a Matrix Technologies micro-Electrapette 25. The measurements were performed while the pipet tip was kept in contact with the drop. The data were collected and averaged over at least three separate slides using two or three drops per slide for each type of SAM. The measured contact angles were always within ±1° of those reported.

PM-IRRAS Measurements. A Nicolet MAGNA-IR 860 Fourier transform spectrometer equipped with a liquid-nitrogen-cooled mercury-cadmium-telluride (MCT) detector and a Hinds Instruments PEM-90 photoelastic modulator operating at 37 kHz was used to collect the PM-IRRAS data. The polarized light was reflected from the sample at an angle of incidence of 80°. The spectra were collected over 64 scans at a spectral resolution of 4 cm^{-1}.

XPS Measurements. XPS spectra were collected using a PHI 5700 X-ray photoelectron spectrometer equipped with a monochromatic Al Kα X-ray source ($h\nu$ = 1486.7 eV) incident at 90° relative to the axis of a hemispherical energy analyzer. The spectrometer was operated at high resolution with a pass energy of 23.5 eV, a photoelectron takeoff angle of 45° from the surface, and an analyzer spot diameter of 1.1 mm. The base pressure in the chamber during measurements was 2×10^{-9} Torr, and the spectra were collected at room temperature. Ten scans were accumulated to obtain the C_{1s} and O_{1s} spectra, while three and twenty scans were accumulated to obtain the Au_{4f} and S_{2p} spectra, respectively. After collecting the data, the binding energies were referenced by setting the $Au_{4f7/2}$ binding energy to 84.0 eV. The peak intensities were quantified by standard curve-fitting software using Shirley background subtraction and Gaussian−Lorentzian profiles.

Results and Discussion

To compare in a systematic manner the SAMs derived from **C*n*C3** to those derived from **C*n*C2** and **C*n***, we propose that SAMs derived from $CH_3(CH_2)_mC(CH_3)[CH_2SH]_2$ correspond to those derived from $CH_3(CH_2)_mCH[CH_2SH]_2$ and $CH_3(CH_2)_{m+2}SH$ as shown in Figure 1. This assumption allows the direct comparison of SAMs in which the number of carbon atoms from the sulfur atom to the terminal methyl group of the longest chain is the same.

Ellipsometry Studies. Measurements of ellipsometric thicknesses allow an estimation of the degree of coverage of SAMs. Due to van der Waals attraction between chains, SAMs having low packing densities will possess alkyl chains with an average orientation that is highly tilted from the surface normal. This extreme chain tilt will in turn give rise to reduced ellipsometric thicknesses compared to those of densely packed SAMs on gold, where the alkyl chains are oriented along the surface normal (albeit with tilt angles as high as 30°).[32] As shown in Figure 3, the ellipsometric thicknesses of the SAMs generated from **C*n*C3** are ~2 Å lower than those generated from **C*n*C2** and ~8 Å lower than those generated from **C*n***. We interpret from these measurements that SAMs generated from **C*n*C3** possess lower chain densities than the corresponding SAMs generated from **C*n*C2** and **C*n***. Consequently, the **C*n*C3** SAMs must possess average alkyl chain orientations that are unique compared to those of the corresponding **C*n*C2** and **C*n*** SAMs.

Specifically, the data suggest that for SAMs derived from **C*n*C3**, the average tilt angle of the alkyl chains is greater than that of SAMs derived from either **C*n*C2** or **C*n***. We use the qualifier "average" because a single angle cannot be representative of all of the alkyl chains in the

(32) Bain, C. D.; Troughton, E. B.; Tao, Y.-T.; Evall, J.; Whitesides, G. M.; Nuzzo, R. G. *J. Am. Chem. Soc.* **1989**, *111*, 321.

Table 1. Advancing (θ_a) and Receding (θ_r) Contact Angles and Hysteresis ($\Delta\theta$) of Water and Hexadecane on SAMs Derived from the Indicated Adsorbates[a]

	C10			C12			C14			C16			C18		
	θ_a	θ_r	$\Delta\theta$	θ_a	θ_r	$\Delta\theta$	θ_a	θ_r	$\Delta\theta$	θ_a	θ_r	$\Delta\theta$	θ_a	θ_r	$\Delta\theta$
							Water								
C*n*	111	102	9	113	103	10	114	103	11	114	104	10	114	104	10
C*n*C2	101	90	11	104	94	10	108	97	11	109	97	12	109	96	13
C*n*C3	98	88	10	103	93	10	106	95	11	106	95	11	106	94	12
							Hexadecane								
C*n*	46	40	6	49	44	5	51	45	6	51	45	6	51	45	6
C*n*C2	16	–	–	22	13	9	29	19	10	33	24	9	42	35	7
C*n*C3	–	–	–	~10	–	–	16	–	–	22	12	10	30	20	10

[a] We report values of at least five independent measurements. Entries marked by (–) were less than 10°, which we define as fully wettable. Values were reproducible within ±1° of those reported.

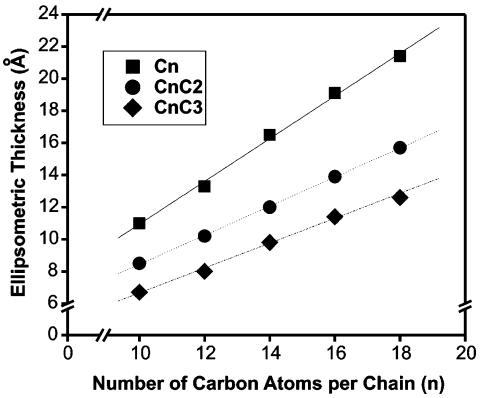

Figure 3. Ellipsometric thicknesses of SAMs generated from **C*n*** (squares), **C*n*C2** (circles), and **C*n*C3** (diamonds).

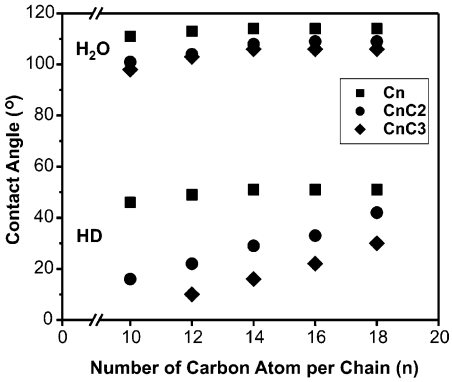

Figure 4. Advancing contact angles of water (H_2O) and hexadecane (HD) on SAMs generated from **C*n*** (squares), **C*n*C2** (circles), and **C*n*C3** (diamonds).

film (see Figure 2). Although we cannot provide an accurate structural model for the loosely packed SAMs, the average tilt angles of alkyl chains in the SAMs can be estimated by plotting the ellipsometric thickness against the number of carbon atoms along the primary chain of the adsorbate (***n***). The slopes in Figure 3 correlate with the film thickness per methylene unit for each adsorbate; consequently, a gentler slope corresponds to a larger average tilt angle. The slope for **C*n*** is 1.3 Å/CH_2, which is in good agreement with the theoretical slope of 1.27 Å/CH_2 calculated using known chain tilts, bond lengths, and bond angles.[32,33] On the other hand, the slopes for **C*n*C2** and **C*n*C3** are 0.92 and 0.77 Å/CH_2, respectively. The observed slopes suggest that the average tilt angles of the alkyl chains in the SAMs increase in the following order: **C*n*** < **C*n*C2** < **C*n*C3**. Given, however, that the refractive indices of the SAMs derived from **C*n*C3** might be different from those derived from the other adsorbates, additional analyses are needed to verify this conclusion.

Contact Angle Studies. Wettability is a highly sensitive tool for probing the structure and composition of surfaces.[30,34] Hexadecane in particular is known to be sensitive to the detailed structure of hydrocarbon interfaces.[23] Table 1 and Figure 4 show uniformly lower contact angles of hexadecane on the **C*n*C3** surfaces (average θ_a = 16°) compared to the **C*n*C2** and **C*n*** surfaces (average θ_a = 28° and 50°, respectively), indicating that hexadecane wets the **C*n*C3** SAMs more than it wets the corresponding **C*n*C2** and **C*n*** SAMs. Given that interfacial methylene groups are more wettable by hexadecane than interfacial methyl groups,[26] the data in Table 1 and Figure 4 suggest that the **C*n*C3** SAMs expose a higher fraction of methylene groups at the surface than do the other two adsorbates. This interpretation is consistent with the average tilt angles inferred from the ellipsometry data (vide supra), which would predict that the SAMs generated from **C*n*C3** should expose more methylene groups on the surface than those generated from **C*n*C2** and **C*n***. The advancing contact angles of water in Table 1 and Figure 4 further support this model, although the effects are less pronounced. The overall results demonstrate that contact angle measurement represents a powerful tool for detecting nanoscale changes in the conformational order of organic thin films, even though it is a macroscopic surface analytical tool.

Table 1 also shows the contact angle hysteresis ($\Delta\theta = \theta_a - \theta_r$), the magnitude of which can be used to evaluate the degree of heterogeneity of interfaces.[30] From the low constant values of $\Delta\theta$ for hexadecane and water, we infer the existence of homogeneously distributed alkyl chains across the interface of all of the SAMs. Additionally, we note that the contact angles of hexadecane on the loosely packed SAMs (**C*n*C3** and **C*n*C2**) progressively increase as a function of chain length (Table 1 and Figure 4). On the other hand, the wetting properties of the **C*n*** SAMs are largely independent of chain length except for the SAM derived from **C10**, which is more wettable than the others. The enhanced wettability of the **C10** SAM likely arises from one or both of the following phenomena. First, the low contact angle for **C10** can be rationalized on the basis of the disordered nature of hydrocarbon SAMs composed of short alkyl chains (i.e., <10 carbon atoms).[32] Second, because the **C10** SAM possesses the shortest chain length of the **C*n*** series, the probe liquid in contact with this SAM is most strongly attracted to the underlying gold substrate via van der Waals forces.[32] Generally,

(33) For calculating the theoretical slope, we assumed that the alkyl chains were fully trans-extended and tilted ~30° from the surface normal. The following data were used: C–C = 1.545 Å, ∠CCC = 110.5°, C–S = 1.81 Å, C–H = 1.1 Å, and the contribution from S was estimated to be 1.5 Å.

(34) Whitesides, G. M.; Laibinis, P. E. *Langmuir* **1990**, *6*, 87.

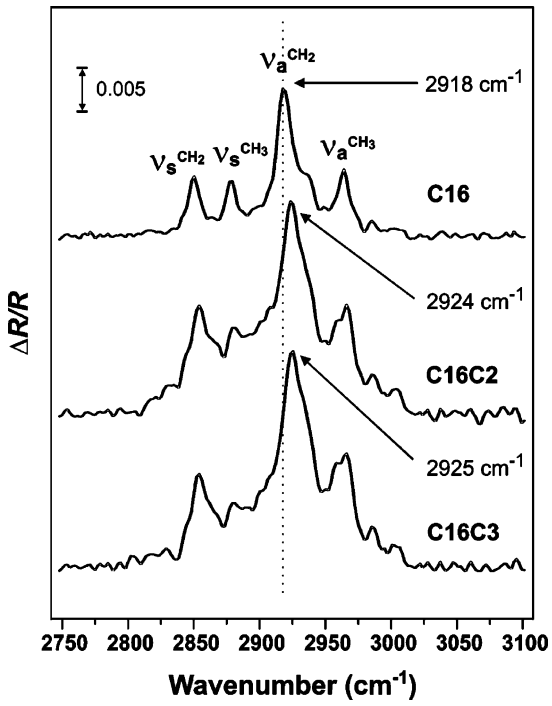

Figure 5. PM-IRRAS spectra of SAMs generated from hexadecanethiol (**C16**), 2-tetradecylpropane-1,3-dithiol (**C16C2**), and 2-methyl-2-tetradecylpropane-1,3-dithiol (**C16C3**).

contact angles are largely constant for *n*-alkanethiol SAMs having chain lengths of >10 carbon atoms.[32] Nevertheless, because (1) all of the SAMs derived from both **C*n*C2** and **C*n*C3** are conformationally disordered to roughly the same extent for all chain lengths examined (vide infra) and (2) the increase in contact angle for the **C*n*C2** and **C*n*C3** SAMs parallels their increase in ellipsometric thickness, we propose that the progressive increase in contact angle with increasing chain length arises from a concomitant decrease in the magnitude of the probe liquid/gold substrate van der Waals interaction (i.e., the contacting drop is positioned progressively further from the gold substrate as the chain length is increased).

PM-IRRAS Studies. Figure 5 shows the C−H stretching regions of the background-corrected PM-IRRAS spectra for the SAMs generated from **C16** and the corresponding chelating alkanedithiols **C16C2** and **C16C3**. The C−H stretching region in the infrared spectra of hydrocarbon SAMs is strongly influenced by the conformation of the alkyl chains and the chain environment.[35] Interpretation of this region follows by assigning the C−H stretching bands (Figure 5),[36,37] which are complicated by Fermi resonance interactions between symmetric fundamental stretching modes and appropriate binary combinations of the methylene bending modes. The shoulder of the methylene antisymmetric stretching band ($\nu_a^{CH_2}$) at ~2935 cm^{-1} has been assigned to the Fermi resonance between the methyl symmetric stretching band ($\nu_s^{CH_3}$) and the methylene bending mode. The methyl antisymmetric stretching band ($\nu_a^{CH_3}$) at ~2965 cm^{-1} consists of both in-plane and out-of-plane antisymmetric modes. However, the surface IR spectra of SAMs usually show only in-plane antisymmetric modes because the out-of-plane antisymmetric mode possesses no dynamic dipole component perpendicular to the surface.[30,38]

Table 2. Band Positions of the Methylene Antisymmetric Stretch ($\nu_a^{CH_2}$) for SAMs Derived from the Indicated Adsorbates[a]

adsorbate	C10	C12	C14	C16	C18
C*n*	2920.9	2920.5	2919.6	2918.2	2918.3
C*n*C2	2923.8	2924.6	2924.2	2924.4	2924.5
C*n*C3	2924.5	2924.8	2925.3	2925.2	2925.1

[a] The $\nu_a^{CH_2}$ band positions were reproducible within ±1 cm^{-1}.

The frequency and the bandwidth of the $\nu_a^{CH_2}$ band are highly sensitive to the conformational order of hydrocarbons.[34,39,40] The band is observed at 2920 cm^{-1} in crystalline *n*-alkanes, which is 8 cm^{-1} lower than that in the liquid state (2928 cm^{-1}).[35] A similar trend has been observed in the infrared spectra of *n*-alkanethiols, where the $\nu_a^{CH_2}$ band position of crystalline *n*-docosanethiol was found at 2918 cm^{-1} while that of liquid *n*-octanethiol was found at 2924 cm^{-1}.[38] In Figure 5, the position of the $\nu_a^{CH_2}$ band at 2918 cm^{-1} is consistent with crystalline conformational order for the **C16** SAM. The $\nu_a^{CH_2}$ band of the SAM derived from **C16C3** is shifted to a substantially higher wavenumber (2926 cm^{-1}), which was also slightly higher than that of the SAM derived from **C16C2** (2925 cm^{-1}).[41] Table 2 shows this same trend of the $\nu_a^{CH_2}$ band positions for all chain lengths investigated.

With respect to chain lengths, the $\nu_a^{CH_2}$ band position for the **C*n*** SAMs decreases from 2920.9 to 2918.3 cm^{-1} as the chain length increases from **C10** to **C18** (Table 2), indicating greater conformational order for the SAMs having longer chain lengths (due to increased interchain van der Waals interactions).[32] In contrast, the respective $\nu_a^{CH_2}$ band positions for the **C*n*C2** and **C*n*C3** SAMs are relatively constant across the entire series of chain lengths ($\nu_a^{CH_2}$ = 2924.2 ± 0.4 and 2924.9 ± 0.4, respectively), indicating their liquidlike conformational order.[42] We interpret from these data that the conformational order of the SAMs decreases in the following order: **C*n*** ≫ **C*n*C2** > **C*n*C3**.[43] The small difference of the $\nu_a^{CH_2}$ band positions for the latter two SAMs (~1 cm^{-1}) is surprising given the large difference in hexadecane contact angles for the **C*n*C3** and **C*n*C2** SAMs (~12°, Table 1). Taken together, the data in Tables 1 and 2 suggest that the $\nu_a^{CH_2}$ band position is highly sensitive to small differences in conformational order for highly ordered SAMs ($\nu_a^{CH_2}$ ~ 2920 cm^{-1}) but surprisingly insensitive for conformationally disordered SAMs ($\nu_a^{CH_2}$ ~ 2925 cm^{-1}).

In Figure 5, we observe a significant increase in the intensities of the methylene stretching bands in loosely packed SAMs (**C16C2** and **C16C3**) when compared with those in the corresponding densely packed analogue (**C16**). The C−H stretching mode intensity in bulk samples is known to decrease with increasing degree of disorder of

(35) Snyder, R. G.; Strauss, H. L.; Elliger, C. A. *J. Phys. Chem.* **1982**, *86*, 5145.
(36) Snyder, R. G.; Hsu, S. L.; Krimm, S. *Spectrochim. Acta* **1978**, *34A*, 395.
(37) MacPhail, R. A.; Strauss, H. L.; Snyder, R. G.; Elliger, C. A. *J. Phys. Chem.* **1984**, *88*, 334.
(38) Porter, M. D.; Bright, T. B.; Allara, D. L.; Chidsey, C. E. D. *J. Am. Chem. Soc.* **1987**, *109*, 3559.
(39) Bensebaa, F.; Ellis, T. H.; Badia, A.; Lennox, R. B. *J. Vac. Sci. Technol., A* **1995**, *13*, 1331.
(40) Bensebaa, F.; Ellis, T. H.; Badia, A.; Lennox, R. B. *Langmuir* **1998**, *14*, 2361.
(41) Although the $\nu_a^{CH_2}$ band positions of the SAMs generated from **C*n*C2** and **C*n*C3** are within our quoted experimental error (±1 cm^{-1}), the $\nu_a^{CH_2}$ band positions of the **C*n*C3** SAMs were reproducibly one wavenumber higher than those of the corresponding **C*n*C2** SAMs.
(42) We note that the $\nu_a^{CH_2}$ band positions for the **C10C2** and **C10C3** SAMs are slightly lower than those of their longer chain analogues (see Table 2). At present, we are unable to rationalize this surprising but experimentally reproducible trend.
(43) Snyder, R. G.; Maroncelli, M.; Strauss, H. L.; Hallmark, V. M. *J. Phys. Chem.* **1986**, *90*, 5623.

Table 3. XPS Binding Energies (eV), Integrated Photoelectron Intensities (Counts), and Relative Chain Densities of SAMs Derived from the Indicated Adsorbates[a]

adsorbate	C_{1s} (eV)	S_{2p} (eV)	Au_{4f} (counts)	C_{1s} (counts)	S_{2p} (counts)	chain density from Au_{4f} (%)	chain density from C_{1s} (%)
C16	285.0	162.1	69 932	8207	446	100	100
C16C2	284.7	162.0	83 159	5962	614	64	64
C16C3	284.7	161.9	85 100	5437	642	58	53
C18	285.0	162.2	64 239	8416	358	100	100
C18C2	284.6	161.9	79 441	6577	560	64	65
C18C3	284.6	161.9	81 277	5952	619	58	54

[a] We report average values of three independent measurements. The binding energies were referenced to $Au_{4f7/2}$ at 84.0 eV. Although the absolute peak areas varied from sample to sample, the calculated chain densities were always within ±3% of those reported.

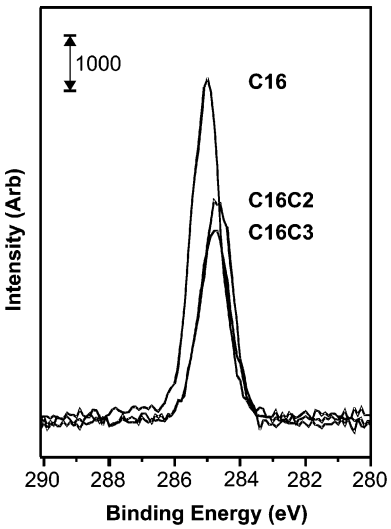

Figure 6. XPS spectra of the C_{1s} region for SAMs generated from hexadecanethiol (**C16**), 2-tetradecylpropane-1,3-dithiol (**C16C2**), and 2-methyl-2-tetradecylpropane-1,3-dithiol (**C16C3**).

alkyl chains.[44] In surface infrared spectra, however, only the component of the dynamic dipole polarized in the direction normal to the surface plane is sensitive. For SAMs on gold with trans-extended alkyl chains (e.g., **C16**), the methylene stretching modes are nearly parallel to the surface.[40] Because gauche defects randomize the orientation of the methylene groups, there is a plausible increase in the number of methylene groups with dipoles perpendicular to the surface for the **C16C2** and **C16C3** SAMs. We caution, however, that the absolute peak intensities obtained via PM-IRRAS measurements can vary from sample to sample unless special precautions are made.[45]

Another feature shown in Figure 5 is the shape of the $\nu_a^{CH_3}$ bands at ~2965 cm^{-1}. For the densely packed **C16** SAM with fully trans-extended alkyl chains, only the in-plane $\nu_a^{CH_3}$ band should be observed according to the surface selection rule.[38] The PM-IRRAS spectra of the loosely packed **C16C2** and **C16C3** SAMs appear to exhibit both in-plane and out-of-plane $\nu_a^{CH_3}$ modes (i.e., split peaks). We propose that the presence of substantial gauche defects and the increased average tilt angles can randomize the orientation of methyl groups, thus allowing the out-of-plane antisymmetric stretching mode to orient perpendicular to the surface. Verification of this hypothesis will require additional experimentation.

XPS Studies. The analysis of SAMs by XPS can reveal information regarding both the chemical composition of the SAMs and the nature of the chemical bond between the adsorbate headgroups and the surface.[46] For SAMs on gold, the latter can be most conveniently evaluated by examining the binding energy of the S_{2p} peak, although spin−orbit coupling can inhibit an accurate analysis.[47] It is known that typical binding energies for the $S_{2p3/2}$ peaks of unbound thiols range between 163 and 164 eV, while those for thiols bound to the gold surface appear at 162 eV.[48] Incomplete adsorbate attachment and/or multilayer formation, therefore, can be identified by the presence of unbound sulfur peaks at ca. 164 eV.[49] Analysis of the SAMs generated from **C16**, **C16C2**, **C16C3**, **C18**, **C18C2**, and **C18C3** by XPS confirms that all of the sulfur atoms are bound to the gold surface and that no oxygen or oxidized sulfur species are present (data not shown). From these studies, we infer complete binding of all sulfur atoms, which remain unoxidized and uncontaminated during SAM formation and characterization.

For SAMs on gold, the binding energy of C_{1s} peaks can be used to provide a rough estimate of the film thickness and/or packing density of alkyl chains on the surface.[50,51] The positive charges generated by photoelectron emission from densely packed SAMs cannot be easily discharged because the adsorbate array acts as an insulator.[51] Loosely packed SAMs, however, are relatively poor insulators; consequently, the C_{1s} binding energy can plausibly shift to lower energies. The shift is unrelated to any changes in chemical state but probably arises due to differing polarizabilities of the SAMs.[50] Figure 6 and Table 3 show a small but reproducible shift of the binding energy of the C_{1s} peaks from 285.0 eV for the **C16** SAM to 284.7 eV for the loosely packed analogues. These data indicate qualitatively that the packing densities of the **C16C2** and **C16C3** SAMs are lower than that of the **C16** SAM. Furthermore, the value of the C_{1s} binding energy can also be used to provide information regarding the orientation of the alkyl chains. Wöll and co-workers reported a significantly diminished C_{1s} binding energy ($\Delta eV = 1.0$ eV) for alkane monolayers oriented parallel versus perpendicular to a metal surface.[52,53] Therefore, the observed 0.3 eV shift to lower binding energy for the C_{1s} peaks of the **C16C2** and **C16C3** SAMs is consistent with more highly tilted alkyl chains compared to those of the **C*n*** SAMs.

(44) Cameron, D. G.; Casal, H. L.; Mantsch, H. H. *Biochemistry* **1980**, *19*, 3665.
(45) Blaudez, D.; Buffeteau, T.; Desbat, B.; Orrit, M.; Turlet, J. M. *Thin Solid Films* **1992**, *210/211*, 648.
(46) Laibinis, P. E.; Whitesides, G. M.; Allara, D. L.; Tao, Y.-T.; Parikh, A. N.; Nuzzo, R. G. *J. Am. Chem. Soc.* **1991**, *113*, 7152.
(47) The S_{2p} peak consists of $2p_{3/2}$ and $2p_{1/2}$ components separated by 1.18 eV with an area ratio of 2:1.
(48) Castner, D. G.; Hinds, K.; Grainger, D. W. *Langmuir* **1996**, *12*, 5083.
(49) Schoenfisch, M. H.; Pemberton, J. E. *J. Am. Chem. Soc.* **1998**, *120*, 4502.
(50) Biebuyck, H. A.; Bain, C. D.; Whitesides, G. M. *Langmuir* **1994**, *10*, 1825.
(51) Ishida, T.; Hara, M.; Kojima, I.; Tsundeda, S.; Nishida, N.; Sasabe, H.; Knoll, W. *Langmuir* **1998**, *14*, 2092.
(52) Himmel, H.-J.; Wöll, Ch.; Gerlach, R.; Polanski, G.; Rubahn, H.-G. *Langmuir* **1997**, *13*, 602.
(53) Witte, G.; Wöll, Ch. *J. Chem. Phys.* **1995**, *103*, 5860.

The packing densities of the SAMs can be more accurately estimated by quantitative calibration of XPS photoelectron intensities. This type of analysis is based on the assumption that the integrated intensities of the Au_{4f} peaks are attenuated by the overlying adsorbate molecules. The relative packing densities of SAMs, therefore, can be obtained by comparing the intensity of the Au_{4f} signal for the SAM of interest with those from a series of *n*-alkanethiol SAMs, whose thicknesses and packing densities are precisely known. The quantitative analysis requires knowledge of the absolute value of the attenuation length. To this end, we plotted the natural logarithm of the Au_{4f} intensities versus the number of carbon atoms in each adsorbate to obtain the attenuation length.[21,54−56] A least-squares analysis of the Au_{4f} signals attenuated by overlying normal alkanethiols (**C10**, **C12**, **C14**, **C16**, and **C18**) showed an attenuation length of 41 Å, in agreement with the value obtained by Bain and Whitesides.[54] We then determined the relative density of chains in the **C*n*C2** and **C*n*C3** SAMs from an "effective" number of carbon atoms per adsorbate, which was derived from the calibration curve generated from the XPS analyses of the *n*-alkanethiol SAMs. Subsequent comparison of this effective number of carbon atoms per adsorbate with the known stoichiometric number of carbon atoms per adsorbate gives the relative density of chains on the surface.[56] Analysis of two separate chain lengths (Table 3) indicates that the packing densities decrease in the following order: **C*n*** ≫ **C*n*C2** > **C*n*C3**. Analysis of the C_{1s} photoelectron intensities[57] gave similar results.

These studies confirm the hypothesis (vide supra) that the low packing density of alkyl chains in the **C*n*C2** and **C*n*C3** SAMs is responsible for the low film thicknesses and loss of conformational order observed by the ellipsometry, contact angle, and PM-IRRAS measurements. Furthermore, the expanded data set for the SAMs generated from **C*n*** and **C*n*C2** are in good agreement with those reported previously.[21] Overall, the results demonstrate that the **C*n*C3** adsorbates generate conformationally disordered monolayer films in which the density of alkyl chains is less than that generated from **C*n*C2** and substantially less than that from **C*n***. Comparison of the data for **C*n*C2** and **C*n*C3** indicates that the substitution of a single hydrogen atom with a methyl group in the adsorbate structure, which represents only a 5% difference in mass, leads to substantial differences in thickness, wettability, conformational order, and surface coverage.

While it is known that the sulfur atoms in **C*n*** SAMs occupy the 3-fold hollow sites on Au(111) surfaces, leading to a sulfur−sulfur spacing of ca. 5 Å,[58,59] none of the data presented here can be used to provide an unequivocal structural model for the binding of the chelating dithiols, **C*n*C2** and **C*n*C3**, to the surface of gold. Nevertheless, given their unique chemical structures and measured packing densities, it seems reasonable to assume for both types of chelating adsorbates that some sulfur atoms bind to 3-fold hollows while others bind elsewhere. A detailed discussion of the packing densities derived from the XPS data for these and related chelating adsorbates will be the subject of a future paper.[60]

Conclusions

A series of new adsorbates, the 2-alkyl-2-methylpropane-1,3-dithiols (**C*n*C3**), were synthesized and used to prepare well-defined SAMs on gold. Characterization of these new SAMs revealed that the **C*n*C3** adsorbates generate uniform monolayer films with low densities of alkyl chains. Moreover, the low density **C*n*C3** SAMs possess alkyl chains that are conformationally disordered and expose a substantial fraction of methylene groups at the interface. Comparison of the **C*n*C3** SAMs to those derived from the known adsorbates **C*n*** and **C*n*C2** revealed the following trend in the packing density and conformational order: **C*n*** ≫ **C*n*C2** > **C*n*C3**. These results demonstrate the key role that molecular design can play in dictating the structure/packing of organic thin films. Future work will target selected structural analogues of **C*n*C3** in which the quaternary methyl group is replaced with a variety of substituents having specifically targeted sizes.

Acknowledgment. The Robert A. Welch Foundation (Grant No. E-1320) and the Texas Advanced Research Program (003652-0307-2001) provided generous support for this research. The authors thank Professor David M. Hoffman for helpful discussions.

LA036424Z

(54) Bain, C. D.; Whitesides, G. M. *J. Phys. Chem.* **1989**, *93*, 1670.

(55) We used the following equation: $\ln(Au_n) = -nd/(\lambda \sin \theta) +$ constant, where Au_n = the Au_{4f} intensity attenuated by a monolayer with *n* carbon atoms, *d* = the thickness of the monolayer per methylene unit (1.1 Å), λ = the attenuation length, and θ = the takeoff angle.

(56) The exact method used for determining the packing densities is described in detail in refs 21 and 27. As in the previous work, we have assumed here that each sulfur atom attenuates the Au_{4f} signal by an amount equivalent to 1.5 carbon atoms.

(57) In this approach, a plot of the C_{1s} intensities versus the stoichiometric number of carbon atoms per adsorbate was used (refs 21 and 27). Since all of the carbon atoms are positioned above the sulfur headgroups, we assume that sulfur exerts no influence on the C_{1s} intensities.

(58) Chidsey, C. E. D.; Liu, G.-Y.; Rowntree, Y. P.; Scoles, G. J. *Chem. Phys.* **1989**, *91*, 4421.

(59) Alves, C. A.; Smith, E. L.; Porter, M. D. *J. Am. Chem. Soc.* **1992**, *114*, 1222.

(60) Park, J.-S.; Vo, A. N.; Barriet, D.; Lee, T. R. Manuscript in preparation.